Five Years Later:

Looking Back at the 2019 Ridgecrest Earthquake Sequence

by Carla Rosa, PG, Tim Dawson, PG, CEG, Kate Thomas, and Alex Morelan, Ph.D., PG
CGS Seismic Hazards Program

IN JULY 2019, two major earthquakes occurred near Ridgecrest, CA: a M6.4 foreshock on July 4th and a M7.1 mainshock on July 5th, known as the Ridgecrest Earthquake Sequence. The causative faults are now known as the Salt Wells Valley and Paxton Ranch fault zones, respectively, which cross each other nearly perpendicularly. The shaking produced by these two events was felt as far away as northern California and central Arizona.

Both earthquakes had widely distributed surface effects, rupturing the ground surface along numerous fault strands and displacing the ground both horizontally and vertically (Rosa et al., 2024). Liquefaction-related deformation features and sand boils also occurred across the region because of the earthquakes.

Field efforts following these two earthquakes allowed for advancements in data collection, such as methods for on-the-ground data acquisition and remote sensing and mapping techniques. Documenting perishable field data following major earthquakes is important for both immediate and long-term fault hazard assessment. This includes using earthquake mapping for swift emergency response soon after the event and to characterize deformation zones for a better understanding of fault mechanics.

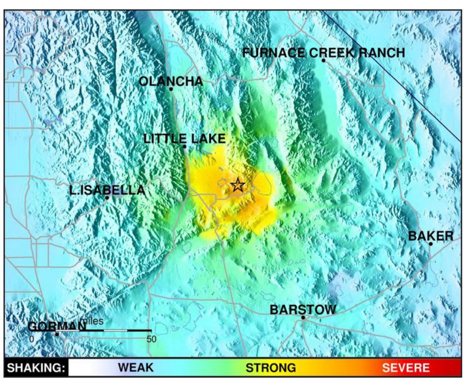

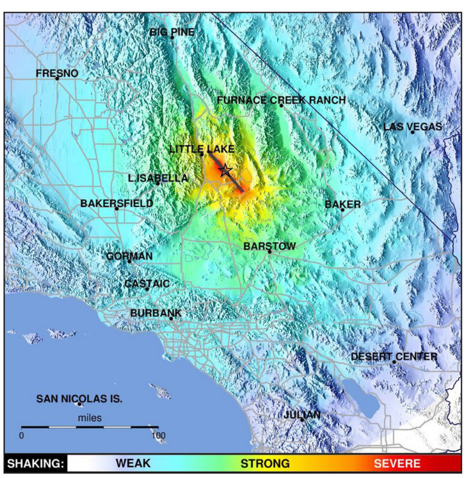

Left: ShakeMaps from the Ridgecrest Earthquake Sequence foreshock on July 4th (top) and the mainshock on July 5th (bottom).

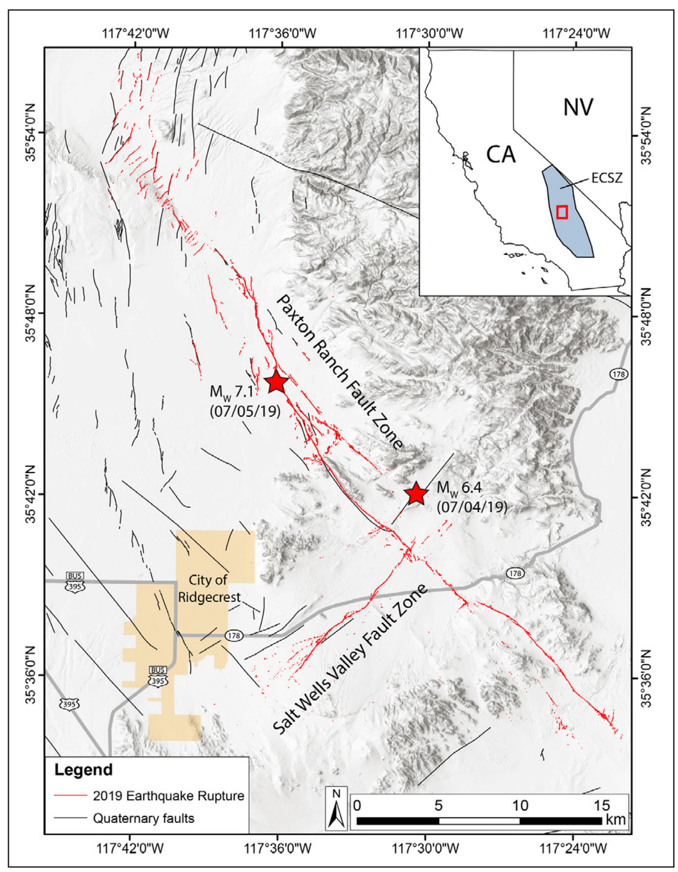

Right: The 2019 Ridgecrest earthquakes ruptured ground along the Paxton Ranch and Salt Wells Valley fault zones (red lines with epicenters marked as red stars) in a zone of known Quaternary aged faults (black lines). These faults comprise a portion of the Eastern California Shear Zone (see inset map). Base source: Airbus, USGS, NGA, NASA, CGIAR, NLS, OS, NMA, Geodatastyrelsen, GSA, GSI and the GIS User Community.

The region where these earthquakes occurred is known as the southern Walker Lane, just north of the Eastern California Shear Zone (ECSZ), both of which help accommodate deformation within the Pacific – North American plate boundary (Wesnousky, 2005). Notable prior historical earthquakes in the region include the 1992 Landers and Big Bear earthquakes, as well as the 1999 Hector Mine earthquake. All of these were located to the southeast of the Ridgecrest earthquakes. The immediate Ridgecrest area has previously experienced smaller earthquake swarms associated with minor ground cracking and displacement since the 1980s.

FIELD RECONNAISSANCE

The Ridgecrest Earthquake Sequence provided a rare opportunity for geologists to observe and document the immediate effects of large earthquakes. The California Geological Survey (CGS) Seismic Hazards Program staff led the initial response to investigate the earthquakes' effects in the field, along with scientists from the United States Geological Survey (USGS) and other scientific agencies and academic institutions. Field response following the 2019 earthquakes included more than 6,000 on-the-ground site observations, of which more than 1,100 included measurements of ground offset, resulting in the mapping of over 68 km (42 miles) of surface rupture produced from both earthquakes (Ponti et al., 2020).

Field mapping and studies following the earthquakes show that the Salt Wells Valley Fault Zone is a mostly continuous, left-lateral fault zone that trends northeast-southwest for approximately 18 km. The largest offset along the Salt Wells Valley Fault Zone is almost 1.6 m of left-lateral movement, observed in the field southwest of the intersection with the Paxton Ranch Fault Zone

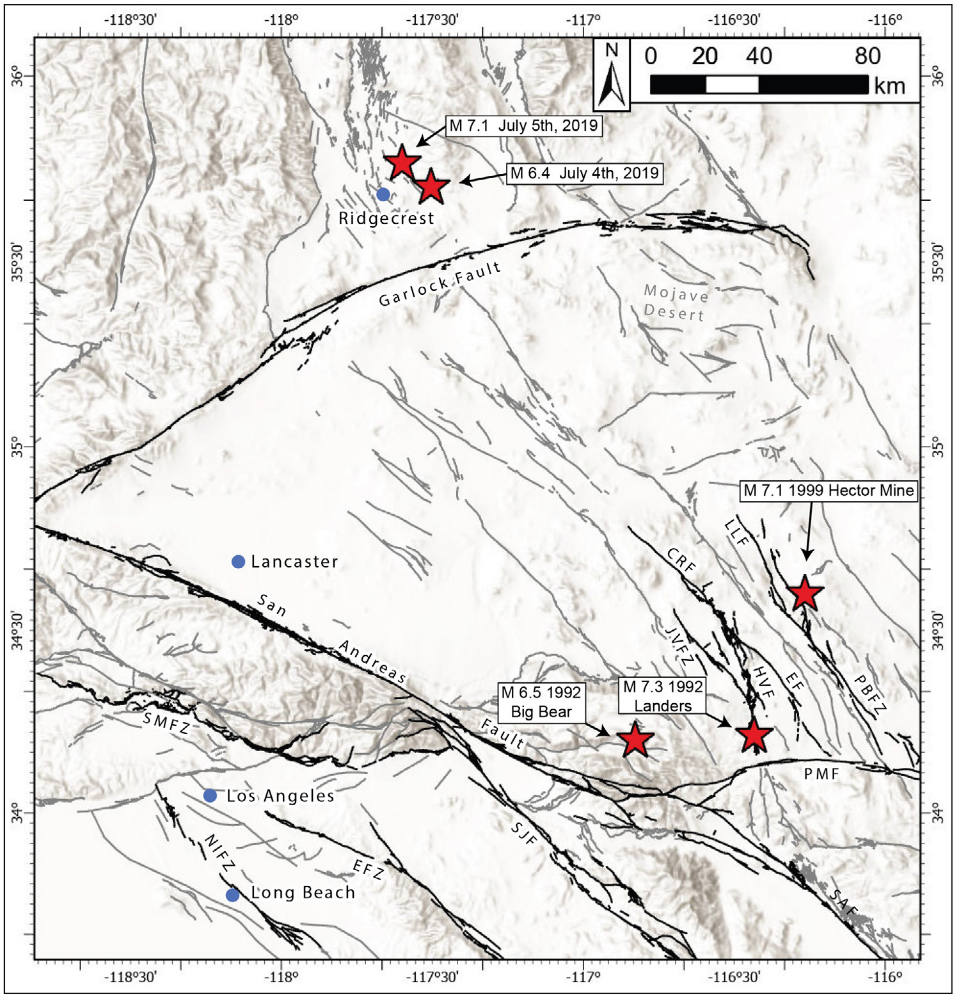

This map shows the 2019 Ridgecrest, the 1992 Landers and Big Bear, and the 1999 Hector Mine epicenters. Thick, black and thin grey lines depict Quaternary age faults. Lavic Lake Fault (LLF); Pisgah-Bullion Fault Zone (PBFZ); Camp Rock Fault (CRF); Emerson Fault (EF); Homestead Valley Fault (HVF); Johnson Valley Fault Zone (JVFZ); Pinto Mountain Fault (PMF); San Jacinto Fault (SJF); Sierra Madre Fault Zone (SMFZ); Newport-Inglewood Fault Zone (NIFZ); Elsinore Fault Zone (EFZ). Source: Quaternary Fault and Fold Database, version 3, USGS and CGS, 2023.

CGS geologist Tim Dawson (in green shirt at top of image) shows U.S. Navy staff surface fault rupture related to the July 5, 2019, M7.1 earthquake on the Paxton Ranch fault. Photo: Ken Hudnut, USGS

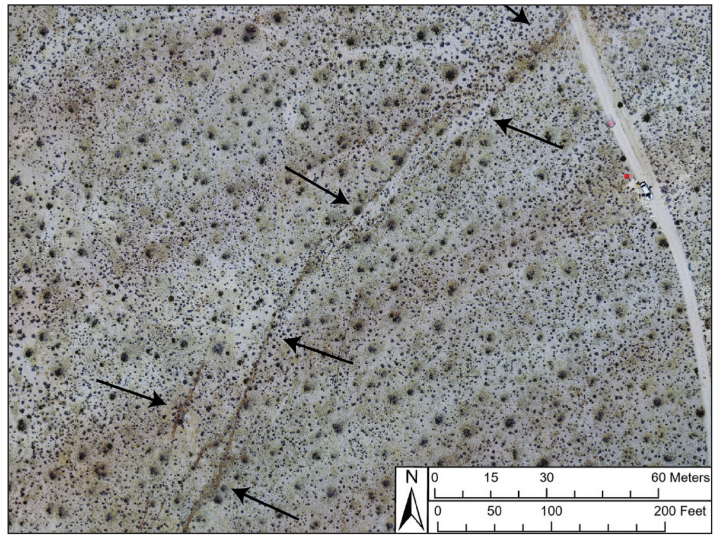

Left image shows Nathaniel Roth preparing to pilot the DJI Matrice 210 for post-earthquake field reconnaissance. Photo by Kate Thomas, CGS.
Right image depicts aerial imagery acquired during post-earthquake field reconnaissance. Black arrows point to trace of surface rupture.

(DuRoss et al., 2020). The Paxton Ranch Fault Zone is characterized by right-lateral movement along a ~50 km (31 miles) long northwest trending fault zone. Right-lateral offsets observed following the M7.1 were as high as 7 m (23 ft) near its epicenter (DuRoss et al., 2020).

ADVANCES IN FAULT MAPPING

Field Reconnaissance

The Ridgecrest Earthquake Sequence provided the CGS with the opportunity to make advances in post-earthquake reconnaissance and fault mapping, such as implementing a digital data acquisition application (Collector for ArcGIS) which facilitated the collection of over 6,000 on-the-ground site observations. This allowed for faster data acquisition, ensured data quality, and provided seamless compilation of those data into a single database. This event also was the first post-earthquake reconnaissance where CGS flew the Da-Jiang Innovations (DJI) Matrice 210 drone to acquire video and images of the surface rupture.

In addition to field data collection advancements, remote mapping of surface rupture and ground deformation features on lidar allowed for a comprehensive and spatially accurate dataset of post-earthquake mapping at a consistent scale that captured previously unmapped features (Rosa et al., 2024). These mapped surface ruptures aided in the creation of Alquist-Priolo Earthquake Fault Zones (APEFZ), which are used for hazard disclosure under the Natural Hazard Disclosure Act and may trigger a geotechnical investigation if development is proposed within the APEFZ.

Remote Sensing Technologies

Optical image correlation is a relatively new method used to document the location and amount the ground moved during an earthquake. This technique involves using pre- and post-earthquake imagery, registered to known locations on the earth, to measure the difference between the two images. A variety of imagery can be used including satellite and aerial images collected from airplanes, helicopters, and/or drones. Following the 2019 Ridgecrest earthquakes,

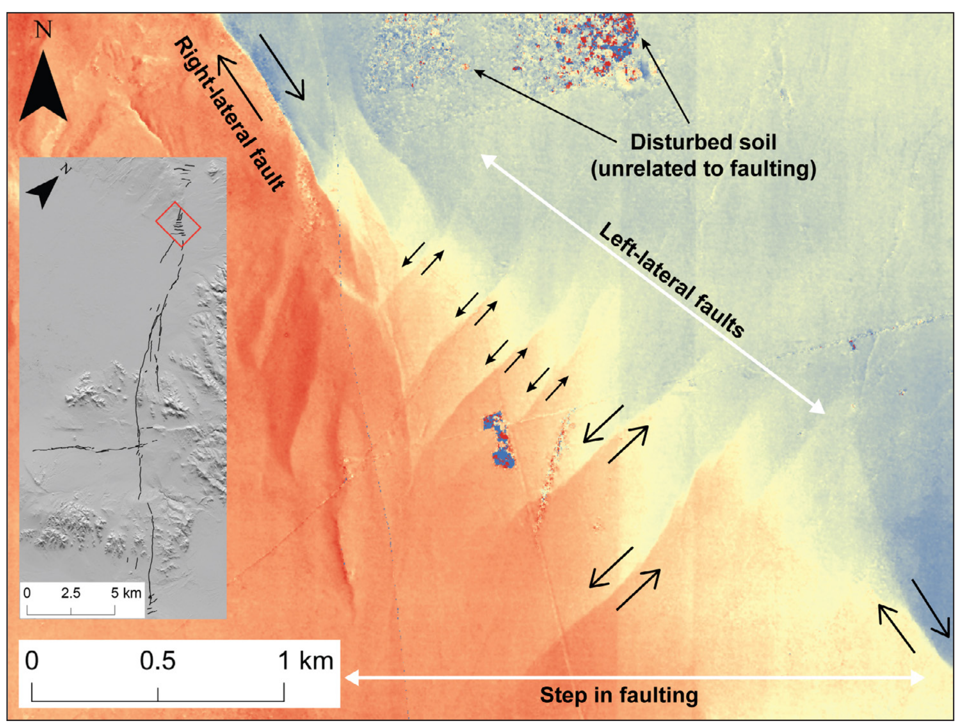

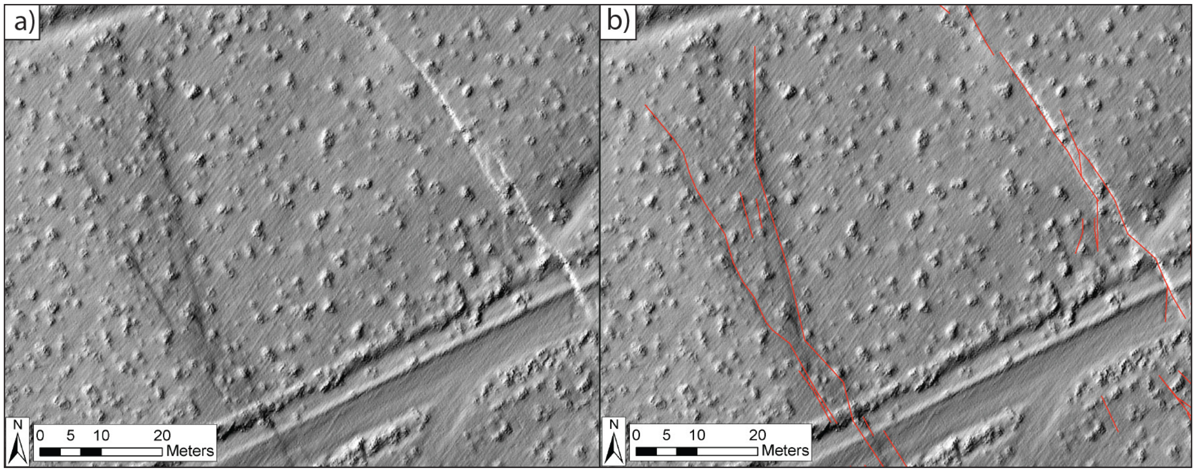

Example of appearance of both east- and west-facing scarps on lidar at 1:700 scale. a) shows features without corresponding mapping; b) shows mapping of features in red. Base is the multi-directional hillshade.

optical image correlation was used to produce maps that highlight the complex patterns of surface faulting that occurred. This technique has great potential to quickly identify where surface deformation has occurred, enabling emergency responders to quickly deploy resources for infrastructure (such as roads, pipelines, buildings) repair (Morelan and Hernandez, 2020).

LEARNING FROM EARTHQUAKES

The 2019 Ridgecrest earthquakes provided an opportunity to collect a rich and unique dataset of observations that can be used to improve our understanding of earthquakes, test new technologies, and ultimately, allow us to better prepare for future earthquakes. Geologists were able to rapidly collect thousands of observations on the ground making this one of the best-documented earthquakes in California. New technologies such as lidar and the use of uncrewed aerial vehicles (UAVs, or drones) were employed to rapidly map the location of surface faulting. Recently developed techniques using satellite imagery and advanced computer processing software showed that surface deformation could be rapidly identified and measured using imagery from before and after the earthquake. These observations are essential in helping emergency managers quickly understand where earthquake damage has occurred following an earthquake and helps them rapidly deploy emergency resources where they are needed most.

Documentation of earthquake effects is also important in improving our understanding of earthquakes. This documentation leads to new and updated earthquake fault zone maps, produced by the CGS to protect the life and safety of Californians (Rosa et al., 2024; see Earthquake Hazard Zones Application (EQ ZApp)). Eventually these post-earthquake studies can lead to improvements in the engineering of buildings, pipelines, and bridges to resist damage during earthquakes.

Opposite page: This map shows displacements near the north end of the 2019 surface rupture as derived from COSI-Corr, an optical image correlation algorithm (Leprince et al., 2009) which utilized National Aerial Imagery Program (NAIP) collected from an airplane as a pre-earthquake baseline image and Pleiades satellite-based imagery as a post-earthquake image to map fault displacements. Inset depicts extent of surface rupture as mapped from COSI-Corr (black lines) and location of main image (red box). The colors in the main image show the magnitudes of movement (red shows relative northward movement and blue shows relative southward movement). Sharp discontinuities in the color ramp are surface-rupturing faults with displacement greater than around 20 cm (8 in). Black arrows show relative movement of the faults that moved during the earthquake. The complexity of faulting is illustrated by the width of deformation, steps in the faulting, and different fault orientations.

REFERENCES

DuRoss, C.B. et al., 2020, Surface displacement distributions for the July 2019 Ridgecrest, California, earthquake ruptures: Bulletin of the Seismological Society of America, v. 110, no. 4, p. 1400-1418, doi:10.1785/0120200058.

Leprince, S., et al., 2009, Co-Registration of optically sensed images and correlation (COSI-Corr): an operational methodology for ground deformation measurements: http://www.tectonics.caltech.edu/slip_history/spot_coseis/ (accessed August 2024).

Morelan, A.E., and Hernandez, J.L., 2020, Increasing postearthquake field mapping efficiency with optical image correlation: Bulletin of the Seismological Society of America, v. 110, no. 4, p. 1419-1426, doi:10.1785/0120200034.

Ponti, D.J. et al., 2020, Documentation of surface fault rupture and ground-deformation features produced by the 4 and 5 July 2019 MW 6.4 and MW 7.1 Ridgecrest Earthquake Sequence, Seismological Research Letters, v.91, no.5, p. 2942-2959, doi:10.1785/0220190322.

Rosa, C.M., 2024, The Paxton Ranch and Salt Wells Valley Fault Zones, with modifications to the Airport Lake and Little Lake Fault Zones in the White Hills, Burro Canyon, Ridgecrest North, Lone Butte, Westend, Spangler Hills West, Spangler Hills East, and Christmas Canyon 7.5-Minute Quadrangles, Inyo, Kern, and San Bernardino Counties, California: California Geological Survey Fault Evaluation Report FER 274, 13 p.

Rosa, C. M., Dawson, T.L., and Kakaria, R., 2024, Surface rupture mapping of the 2019 M6.4 and M7.1 Ridgecrest Earthquake Sequence on Lidar and orthoimagery: California Geological Survey Special Report 257, 37 p.

Wesnousky, S.G., 2005, Active faulting in the Walker Lane: Tectonics, v. 24, no. 3, 35 p., doi:10.1029/2004TC001645.